Performance enhancement of Brillouin optical correlation domain analysis based on frequency chirp magnification

Bin Wang (王 彬), Xinyu Fan (樊昕昱)*, Jiangbing Du (杜江兵), and Zuyuan He (何祖源)

State Key Laboratory of Advanced Optical Communication Systems and Networks, Shanghai Jiao Tong University, Shanghai 200240, China

**Corresponding author: fan.xinyu@sjtu.edu.cn*

Received July 17, 2017; accepted September 22, 2017; posted online November 2, 2017

We propose a method to enhance the performance of Brillouin optical correlation domain analysis (BOCDA) with a broad chirp span of optical sources based on the frequency chirp magnification technique. In BOCDA systems, the number of effective sensing points is proportional to the chirp span of the light source, which is normally limited by the characteristics of the laser diode. We demonstrate a chirp span of 126 GHz with the proposed method, to double the effective sensing points of BOCDA. By combining with differential measurement schemes, a spatial resolution of <10 cm over a 1 km range is achieved.

OCIS codes: 060.2370, 290.5900, 190.4380.

doi: 10.3788/COL201715.120601.

Distributed fiber-optic sensing technology is now attracting considerable attention in many fields since it provides continuous information along the whole fiber used for sensing applications. To realize the distributed measurement for locating the "event," there are three main methods using different locating principles in different domains: time, frequency, and correlation[1–3]. Among these methods, the time-domain locating technique is widely used due to its cost effectiveness and long measurement distance[4–8]. Several sensing systems using the time-domain locating technique, such as optical time-domain reflectometry (OTDR) and Brillouin optical time-domain analysis (BOTDA), achieved great successes in many applications[9–11], such as border security monitoring, oil pipeline monitoring, etc. However, the spatial resolution of the time-domain method is limited to meter level because of the poor signal-to-noise ratio (SNR) when a narrow optical pulse is launched into the fiber under test (FUT), which refrains from meeting the requirements of high-resolution measurements and restricts its applications. On the contrary, the frequency-domain method can achieve high spatial resolution[12,13], but it has a limited measurement range since it is susceptible to the phase noise of the optical source and the accumulated phase noise from the FUT added by the environmental perturbations along the fiber.

The correlation-domain method, which provides ultrahigh (millimeter-level) spatial resolution and a relatively long measurement range[14–17], is another possible substitute for the time-domain method and frequency-domain method. It is based upon a reflectometric technique called the synthesis of optical coherence function (SOCF)[18,19]. In this method, the optical frequency of the laser diode (LD) is modulated, usually step by step or sinusoidal, by controlling the current injected into the LD. The spatial resolution of correlation-domain sensing systems is inversely proportional to the chirp span of the light source, and a broader bandwidth helps to obtain a higher spatial resolution. For the typical sinusoidal modulation, a broad modulation bandwidth can be obtained by increasing the current injected into the LD. However, the increase of injection current added risks of damaging the LD, and the modulation bandwidth is usually less than 60 GHz[20,21].

In this Letter, we propose a method to improve the spatial resolution of Brillouin optical correlation domain analysis (BOCDA) based on frequency chirp magnification (FCM) by using the four-wave-mixing (FWM) process in highly nonlinear fiber (HNLF)[22,23]. In the FWM process, when the pump has a frequency chirp, the generated idlers also have a frequency chirp but the span is magnified[24]. The broadened frequency span helps to obtain a high performance (high spatial resolution or more effective sensing points) in correlation-domain sensing systems. In BOCDA systems, the maximum chirp span of the LD is ~63 GHz (90 kHz modulation frequency), and the span of the generated Idler-1 is broadened to ~126 GHz, which is the largest chirp span ever reportedly achieved in BOCDA systems. We have doubled the number of effective sensing points from 3300 to 6600, and achieved a spatial resolution of 17 cm over a 1 km measurement range. We believe that higher performance can be obtained by generating higher-order idlers or utilizing a cascaded FWM process. Moreover, the capability of combining different performance-enhancing techniques in BOCDA is also verified. By combining the FCM technique with the differential measurement scheme[25–27], a spatial resolution of <10 cm over a 1 km measurement range is obtained. We believe that the proposed technique may be introduced into the state-of-the-art BOCDA systems to achieve more than one million effective sensing[28,29].

In conventional BOCDA systems, the frequency of the light source is sinusoidal modulated to generate periodical coherence peaks (CPs). The measurement range

corresponds to the interval between two adjacent CPs, and can be given by[30]

$$d_m = c/(2nf_m), \tag{1}$$

where c and n are, respectively, the light velocity in a vacuum and the effective refractive index of the fiber, and f_m is the modulation frequency of the LD. The spatial resolution of the system can be expressed by[30]

$$\Delta d = c\Delta v_B/(2\pi n f_m \Delta f), \tag{2}$$

where Δv_B is the Brillouin gain bandwidth of the FUT, and Δf is half of the chirp span of the laser source. The number of effective sensing points N_{eff} is defined as the ratio of the measurement range and the spatial resolution, and can be given by

$$N_{\text{eff}} = d_m/\Delta z = \pi\Delta f/\Delta v_B. \tag{3}$$

According to Eq. (3), N_{eff} is proportional to Δf, which means that a broad frequency modulation span helps to increase the effective sensing points in the BOCDA system. Since Δf is normally limited by the characteristics of the LD, it is proposed to be broadened by using the FCM technique, which is achieved by using the FWM process in HNLF.

Figure 1 shows the schematic illustration of the FWM process. The generated Idler-1 has an electric field E_i described by

$$E_i = CA_p^2 A_s \exp[j(2\omega_p - \omega_s)t + 2(f_p - f_s)], \tag{4}$$

where ω_p, ϕ_p, and A_p are, respectively, the frequency, phase, and amplitude of the pump; ω_s, ϕ_s, and A_s are, respectively, the frequency, phase, and amplitude of the seed; C is a constant related to the FWM efficiency. After the FWM process, the pump, the seed, and Idler-1 will have a frequency relationship given by $\omega_{i-1} = 2\omega_p - \omega_s$. For a pump with a frequency modulation span of $\Delta\omega$, the obtained Idler-1 has a frequency of $2(\omega_p + \Delta\omega) - \omega_s$. Therefore, the modulation span of Idler-1 is doubled compared to that of the pump. Similarly, the frequency of Idler-2 can be described as $\omega_{i-2} = 3(\omega_p + \Delta\omega) - 2\omega_s$, and its modulation span is broadened to three times that of the pump. Much wider frequency modulation spans can be realized by generating higher-order idlers or utilizing a cascaded FWM process. The generated idler, which has a wide frequency chirp span, can be used in BOCDA systems to improve their performance.

The experimental setup of the proposed FWM-enhanced BOCDA system is shown in Fig. 2. A distributed feedback (DFB) laser with a sinusoidal current modulation is employed as the pump, and a fiber laser is used as the seed. The optical power of the pump is amplified to 50 mW by an erbium-doped fiber amplifier (EDFA), and the output power of the seed is 40 mW. The pump and the seed are combined by a coupler and then launched into the HNLF. The generated Idler-1 is filtered out and utilized as the light source for the BOCDA system. The Brillouin gain spectrum (BGS) is measured by sweeping the RF signal applied to the single-sideband modulator (SSBM) with frequencies near 11 GHz. Two EDFAs are used to amplify the pump power and probe power to 21 and 10 dBm, respectively. The modulation frequency of the light source is near 95 kHz, which corresponds to a measurement range of ~1100 m. The length of FUT is ~1 km, and the delay-fiber length is ~10 km. The CP located in FUT is moved by changing the modulation frequency f_m. In the experiment, a polarization scrambler (PS) is utilized to mitigate the polarization-dependent gain fluctuation. A photodiode (PD) is used as a detector, and the BGS data are obtained from a lock-in amplifier (LIA) connected to the PD. Two types of LIA methods, the intensity modulation (IM) method and the phase modulation (PM) method, are used in the BOCDA system, respectively. The chopping frequency for the IM method is 311 kHz, while the modulation frequency for the PM method is $f_m/4$. The Brillouin signals are collected by an analog-to-digital converter and then digitally processed using a personal computer.

As shown in Fig. 3, the modulation span of the pump is about 63 GHz (corresponding to a spatial resolution of 34 cm), and the optical chirp span of the generated

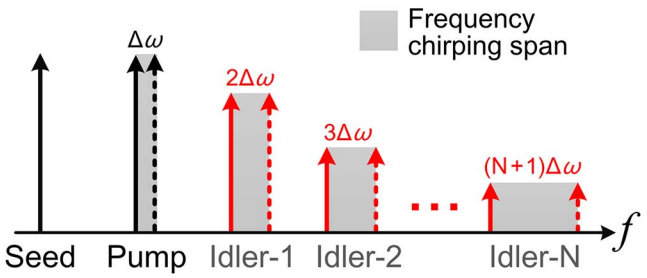

Fig. 1. Schematic illustration of optical frequency modulation span broadening based on the FCM technique by using the FWM process. $\Delta\omega$ is the modulation span of the pump.

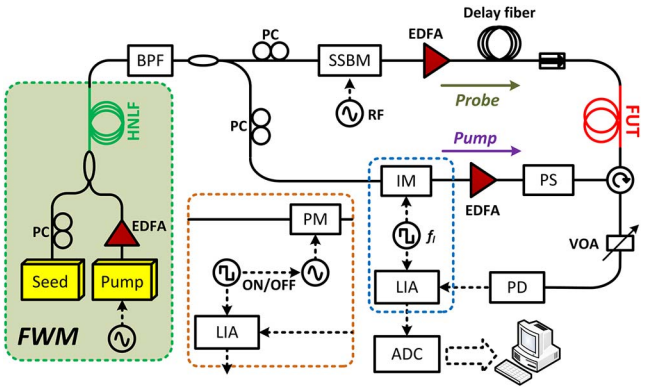

Fig. 2. Experimental setup of the proposed BOCDA system based on the FCM technique. BPF: bandpass filter; VOA: variable optical attenuator; ADC: analog-to-digital converter.

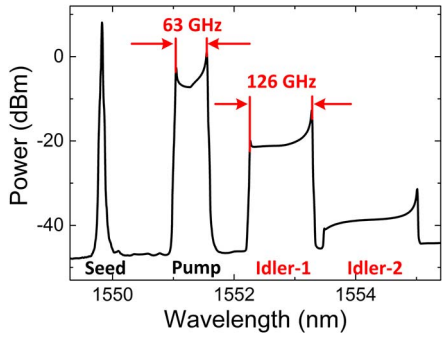

Fig. 3. Measured optical spectrum after the FWM process at the end of the HNLF.

Idler-1 is broadened to 126 GHz (corresponding to a spatial resolution of 17 cm), which is the largest chirp span ever reportedly achieved in BOCDA systems. Although the second-order idler (chirp span of ~190 GHz) can be observed, its optical power is too low so that it cannot be used as the light source of the BOCDA system. Some FWM efficiency-enhancing methods, including optical feedback and multistage mixers[31,32], can be used to generate higher-order idlers to obtain broader chirp span. The pump shown in Fig. 3 has an asymmetric optical spectrum caused by the parasitic IM of the DFB laser[33]. The parasitic IM is amplified for the Idler-1 since its power is proportional to the square of the pump power, as given in Eq. (4), which leads to a slight spectrum distortion. Fortunately, the adverse effect caused by the spectrum distortion can be ignored in BOCDA since the parasitic IM is very small and has very few influences on the BGS.

To verify the performance enhancement of the proposed technique experimentally, the pump and the Idler-1 are respectively filtered out to be used as the light source of BOCDA system. The theoretical spatial resolutions are 34 cm for the pump and 17 cm for Idler-1. A 20-cm-long dispersion-shift fiber (DSF), whose Brillouin frequency shift (BFS) is near 200 MHz downshifted from the single-mode fiber (SMF), is spliced to the end of a 1-km-long SMF. Figures 4(a) and 4(b) give the 3D plot of the distributed BGS around the end of the FUT when

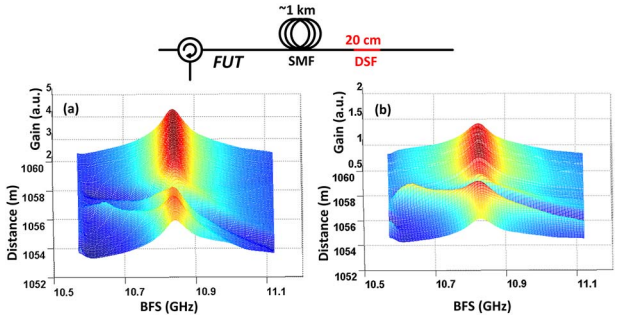

Fig. 4. 3D plot of the distributed BGS around the end of the FUT when (a) the pump and (b) Idler-1 are used as the light source of the BOCDA system, respectively.

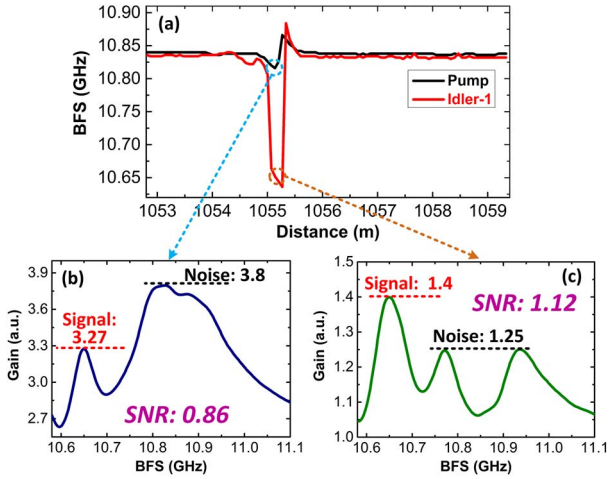

Fig. 5. (Color online) (a) Distribution map of the BFS measured with the pump and Idler-1; the measured BGS of the DSF when (b) the pump and (c) Idler-1 are used as light source, respectively.

the pump and Idler-1 are respectively used as the light source. The distribution map of the BFS is shown in Fig. 5(a), and the DSF cannot be recognized when the pump is used as the light source since the length of the DSF (20 cm) is shorter than the theoretical spatial resolution (34 cm). When Idler-1 is used as the light source, the BFS of the DSF can be correctly measured since Idler-1 has a broader chirp span, sufficient to provide a higher spatial resolution (17 cm). Figures 5(b) and 5(c) show the BGS of the DSF section measured with the pump and Idler-1. The SNR is 0.86 with the pump, showing why the 20 cm DSF section cannot be successfully measured, and it is improved to 1.12 when Idler-1 is used in the BOCDA system. Based on the FCM technique by using the FWM process, we doubled the effective sensing points of the BOCDA system from 3300 to 6600. Here we observe that the bandwidth of the measured BGS is slightly broader when Idler-1 is used as the light source resulted by the wavelength dependence of the Brillouin frequency, which may deteriorate the measurement accuracy. This problem can be solved by using the differential measurement technique to narrow the BGS bandwidth.

The proposed FCM technique can be combined with other performance-enhancing techniques used in the BOCDA system, such as the temporal gating scheme and differential measurement technique, to achieve an extreme performance. In our experiments, we combine the FCM technique with the differential measurement technique, and achieved a spatial resolution of <10 cm over a 1 km measurement range. Figure 6(a) shows 3D plot of the distributed BGS around the end of the FUT. The corresponding BFS is given in Fig. 6(b), and the DSF section can be clearly recognized. The insets give the BGSs of the SMF section and the DSF section, which are centered at different frequencies. We believe that the proposed FCM technique can be used as an additional technique for realizing more effective sensing points in the state-of-the-art BOCDA system.

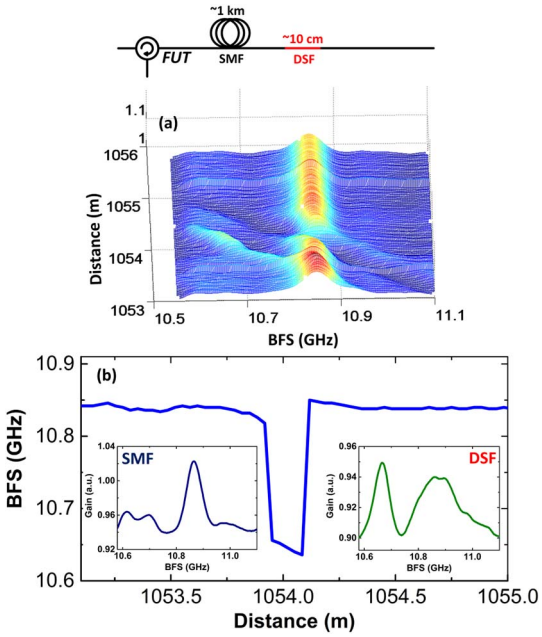

Fig. 6. (a) 3D plot of the distributed BGS around the end of the FUT. (b) The measured BFS around the 10 cm DSF section with differential measurement techniques. The insets show the BGS of the SMF and DSF.

In conclusion, a method based on FCM by using the FWM process in HNLF to improve the performances of BOCDA is proposed. By utilizing the FWM process to generate idler light waves, we demonstrate a wide chirp span of up to 126 GHz. By utilizing the generated idler as the light source, the effective sensing points of BOCDA are doubled from 3300 to 6600. Moreover, we also experimentally verify the capability of combining the FCM technique with other performance-enhancing schemes to a achieve higher sensing performance. By combining with the differential measurement scheme, a spatial resolution of <10 cm over a 1 km measurement range is obtained. We believe that the proposed technique can be introduced into state-of-the-art BOCDA systems to achieve more than one million effective sensing points.

The work was supported by the National Key R&D Program of China under Grant No. 2017YFB0405500.

References

1. M. K. Barnoski, M. D. Rourke, S. M. Jensen, and R. T. Melville, Appl. Opt. **16**, 2375 (1977).
2. H. Barfuss and E. Brinkmeyer, J. Lightwave Technol. **7**, 3 (1989).
3. K. Hotate and O. Kamatani, J. Lightwave Technol. **11**, 1701 (1993).
4. M. Soto, M. Taki, G. Bolognini, and F. Pasquale, IEEE Photonics Technol. Lett. **24**, 1823 (2012).
5. M. Soto, G. Bolognini, and F. Pasquale, Opt. Lett. **36**, 2 (2011).
6. Z. Wang, X. Jia, H. Wu, F. Peng, Y. Fu, and Y. Rao, Proc. SPIE **10323**, 103230T (2017).
7. Y. Dong, L. Chen, and X. Bao, J. Lightwave Technol. **30**, 8 (2012).
8. Y. Dong, L. Chen, and X. Bao, Opt. Lett. **36**, 2 (2011).
9. Z. Wang, Z. Pan, Q. Ye, B. Lu, Z. Fang, H. Cai, and R. Qu, Chin. Opt. Lett. **13**, 100603 (2015).
10. F. Peng, H. Wu, X. Jia, Y. Rao, Z. Wang, and Z. Peng, Opt. Express **22**, 11 (2014).
11. Y. Peled, A. Motil, I. Kressel, and M. Tur, Opt. Express **21**, 10697 (2013).
12. B. Soller, D. Gifford, and M. Wolfe, Opt. Express **13**, 666 (2005).
13. R. Bernini, A. Minardo, and L. Zeni, IEEE Photonics J. **4**, 48 (2012).
14. K. Y. Song, Z. He, and K. Hotate, Opt. Lett. **31**, 17 (2006).
15. K. Y. Song, Z. He, and K. Hotate, in *Optical Fiber Sensors* (2006), paper ThC2.
16. J. Chai, M. Zhang, Y. Liu, L. Li, W. Xu, and Y. Wang, Chin. Opt. Lett. **13**, 080604 (2015).
17. M. Zhang, X. Bao, J. Chai, Y. Zhang, R. Liu, H. Liu, Y. Liu, and J. Zhang, Chin. Opt. Lett. **15**, 080603 (2017).
18. K. Hotate, Meas. Sci. Technol. **13**, 1746 (2002).
19. K. Hotate and Z. He, J. Lightwave Technol. **24**, 7 (2006).
20. M. Shizuka, N. Hayashi, and Y. Mizuno, Appl. Opt. **55**, 3925 (2016).
21. M. Shizuka, S. Shimada, N. Hayashi, Y. Mizuno, and K. Nakamura, Appl. Phys. Express **9**, 032702 (2016).
22. B. P. -P. Kuo and S. Radic, Opt. Express **18**, 19 (2010).
23. M. Badar, H. Kobayashi, and K. Iwashita, IEEE Photonics Technol. Lett. **28**, 1680 (2016).
24. J. Du and Z. He, Opt. Express **21**, 22 (2013).
25. J. H. Jeong, K. Lee, K. Y. Song, J. Jeong, and S. B. Lee, Opt. Express **20**, 24 (2012).
26. J. H. Jeong, K. H. Chung, S. B. Lee, K. Y. Song, J. Jeong, and K. Lee, Opt. Express **22**, 2 (2014).
27. R. Shimizu, M. Kishi, and K. Hotate, Proc. SPIE **10323**, 103239O (2017).
28. Y. H. Kim, K. Lee, and K. Y. Song, Opt. Express **23**, 26 (2015).
29. G. Ryu, G. T. Kim, K. Y. Song, S. B. Lee, and K. Lee, Proc. SPIE **10323**, 1032369 (2017).
30. K. Hotate and K. Kajiwara, Opt. Express **16**, 7881 (2008).
31. E. Myslivets, B. P.-P. Kuo, N. Alic, and S. Radic, Opt. Express **20**, 3331 (2012).
32. J. Li, X. Xiao, L. Kong, and C. Yang, Opt. Express **20**, A20 (2012).
33. K. Y. Song, Z. He, and K. Hotate, J. Lightwave Technol. **25**, 5 (2007).